Science Advances
AAAS

Supplementary Materials for

Sequential maturation of stimulus-specific adaptation in the mouse lemniscal auditory system

Patricia Valerio *et al.*

Corresponding author: Tania Rinaldi Barkat, tania.barkat@unibas.ch

Sci. Adv. **10**, eadi7624 (2024)
DOI: 10.1126/sciadv.adi7624

This PDF file includes:

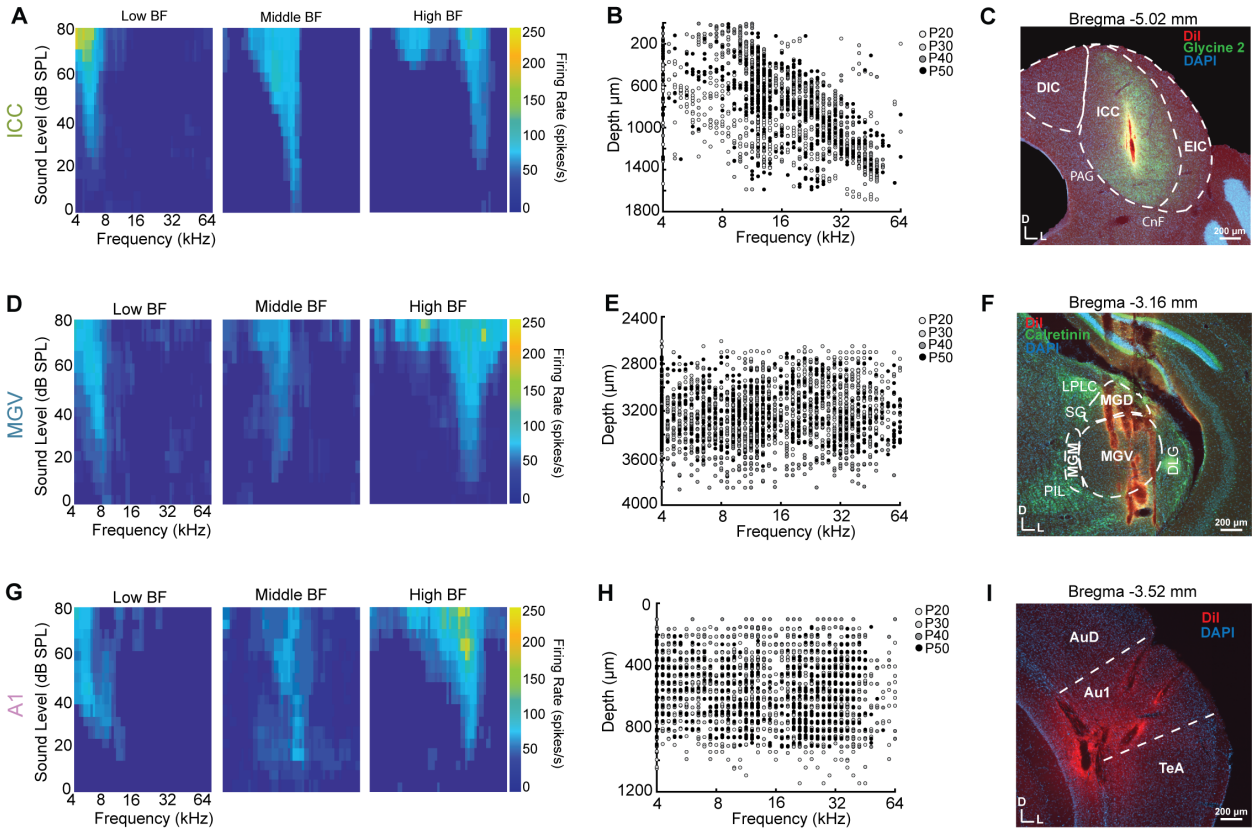

Fig. S1. Functional and anatomical identification of ICC, MGV, and A1. (**A, D, G**) Representative frequency response area (FRA) of low-, middle-, and high-BF tuned cells in ICC, MGV, and A1, respectively. Pure tones of varying frequency and sound levels used to determine the FRAs. Color code represents the firing rate (spikes/s), with higher values represented with brighter colors. (**B, E, H**) Distribution of BFs along the probe from the pia surface (µm) for P20, P30, P40, and P50 groups. Positive identification of ICC and A1 through their tonotopic map (IC: dorso-ventral, low to high BF; A1: caudo-rostral, low to high BF). MGV location based on the auditory responses. (**C, F, I**) Representative image of right hemisphere coronal slice for IC, MGB, and A1, respectively. Single-shaft electrode inserted in ICC, and 4-shaft in MGV and A1, tracked using DiI dye (red). To differentiate IC divisions, antibody used against Glycine 2 transporter (green; highly expressed in ICC). For MGB, an antibody against Calretinin (green) allowed identification of different divisions (not expressed in MGV). Cell nuclei stained with DAPI (blue). 10x magnification. Scale 200 µm. DIC, dorsal IC. ICC, central IC. EIC, external IC. PAG, periaqueductal grey. CnF, cuneiform nucleus. MGV, ventral MGB. MGD, dorsal MGB. MGM, medial MGB. LPLC, lateral posterior thalamic nucleus. SG, suprageniculate thalamic nucleus. PIL, posterior intralaminar thalamic nucleus. DLG, dorsal lateral geniculate nucleus. Au1, primary auditory cortex. AuD, secondary auditory cortex. TeA, temporal association cortex. D, dorsal. L, lateral.

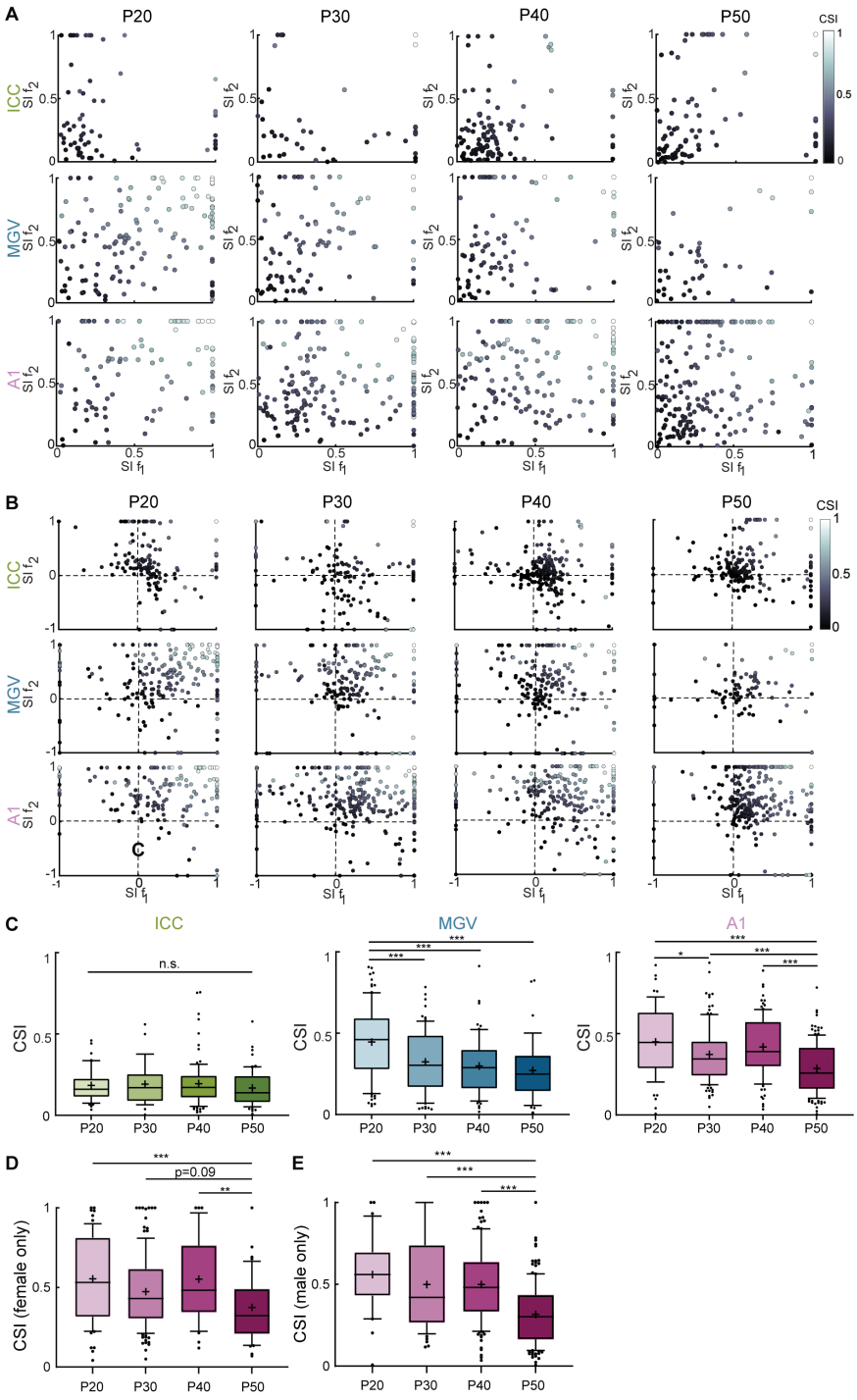

Fig. S2. Hierarchical SSA across central auditory areas during adolescence.
(**A**) Scatter plot of SI f_1 and SI f_2 for ICC, MGV, and A1, respectively. Only units with SI> 0 were selected for analysis. The color code represents CSI (black to white: low to high). (**B**) Scatter plot of SI f_1 and SI f_2 for ICC, MGV, and A1 P20, P30, P40, and P50. All cells are represented. ICC: P20, 218 cells; P30, 226 cells; P40, 295 cells; P50, 261 cells. MGV: P20, 269 cells; P30, 208 cells; P40, 275 cells; P50, 121 cells. A1: P20, 225 cells; P30, 434 cells; P40, 340 cells; P50, 346 cells. Color code gradient CSI (black to white: low to high). (**C**) Average CSI for ICC, MGV, and A1,

respectively, SI>0 and SI<1 cells selected for analysis. ICC: P20, 48 cells; P30, 28 cells; P40, 95 cells; P50, 60 cells; f=0.58, df=230. MGV: P20, 97 cells; P30, 75 cells; P40, 64 cells; P50, 38 cells; f=11.31, df=273. A1: P20, 59 cells; P30, 118 cells; P40, 103 cells; P50, 137 cells; f=17.54, df=416. (**D, E**) CSI in A1 as a function of age for female (D; P20, n=4 mice, 65 cells; P30, n=4 mice, 129 cells; P40, n=1 mouse, 34 cells; P50, n=3 mice, 43 cells; ***, p=0.001, **, p=0.0075; f=5.85 df=270) and male (E; P20, n=3 mice, 31 cells; P30, n=2 mice, 54 cells; P40, n=4 mice, 120 cells; P50, n=4 mice, 140 cells; ***, p<0.001; f=21.45 df=344) mice. one-way ANOVA with multiple comparisons. In the boxplots, lines represent median, 25^{th} and 75^{th} percentiles, + represents mean, whiskers represent 10^{th} and 90^{th} percentiles, and points below or above the whiskers are drawn as individual points.

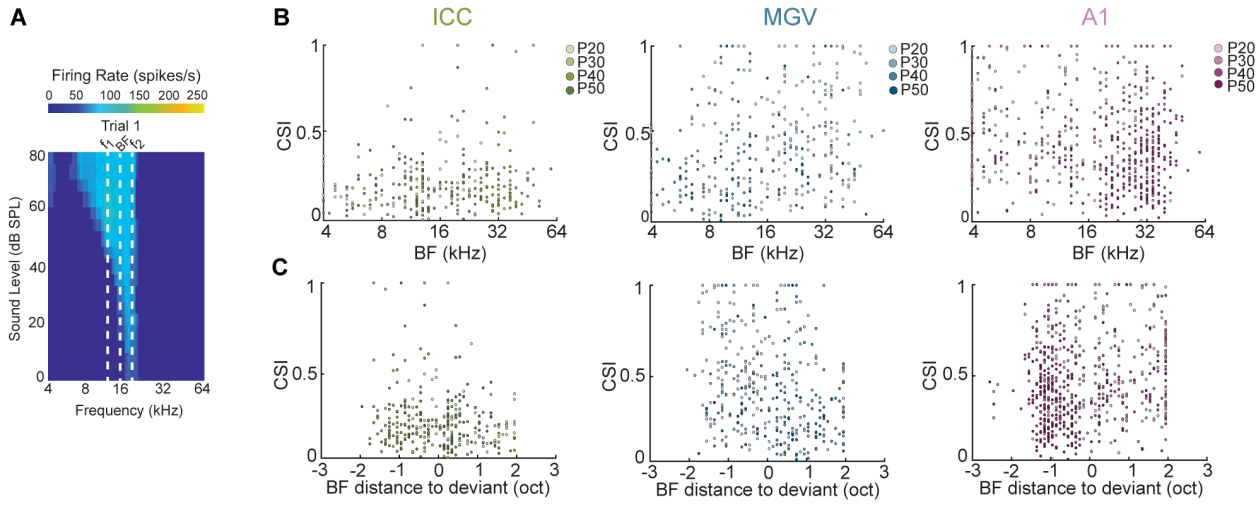

Fig. S3. SSA changes do not correlate with BF or f_1 and f_2 distributions. (**A**) Representative frequency response area (FRA) of recorded units. The vertical dashed white lines represent the chosen f_1 and f_2 frequencies 0.5 octaves apart, the cell's best frequency (BF). The color code represents the firing rate (spikes/s), with higher values represented with brighter colors. (**B**) Scatter plot of CSI vs. BF of units for each area and age group. (**C**) Scatter plot of CSI vs. BF distance to the deviant tone. Color code as in Fig. 1.

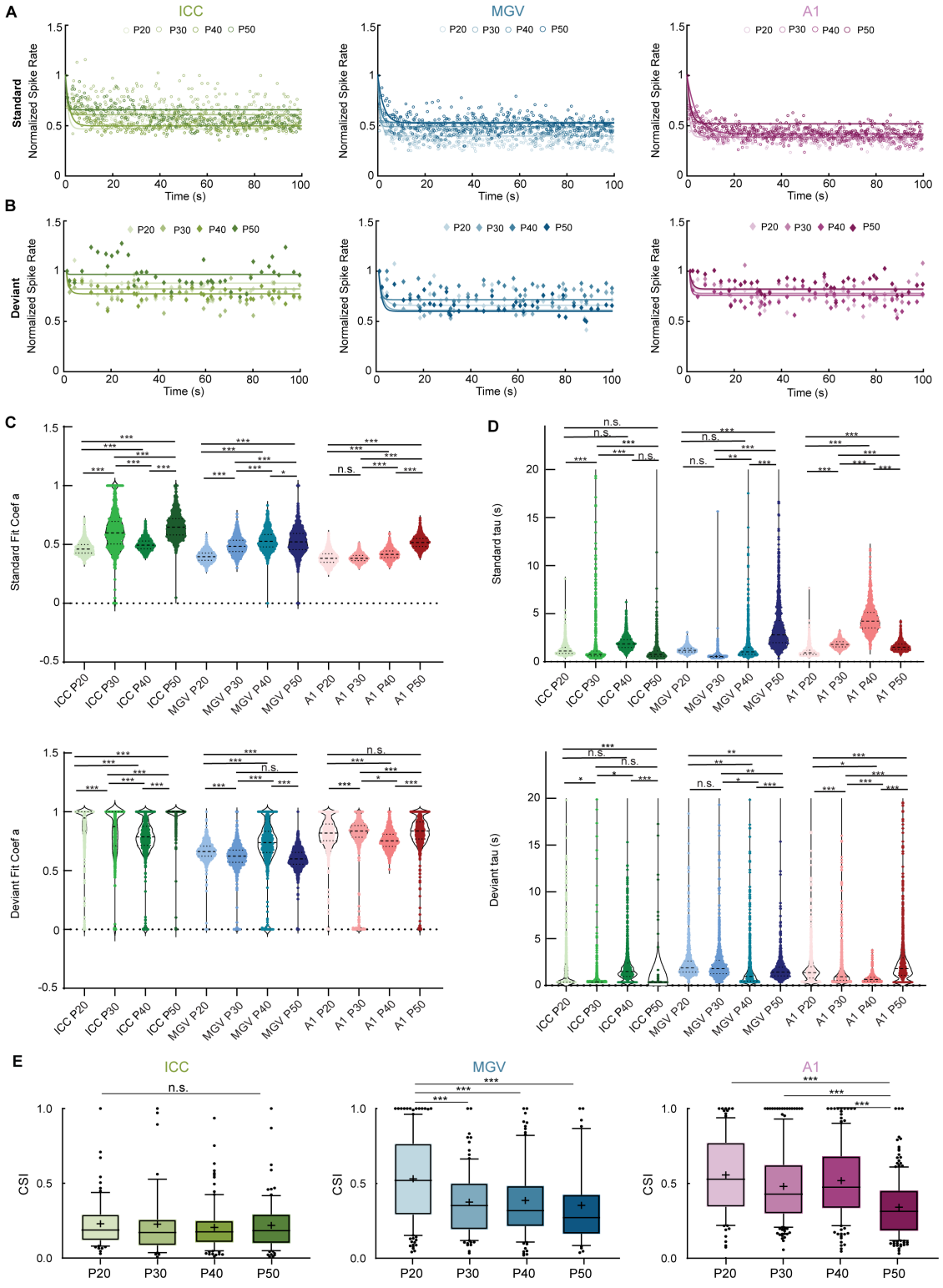

Fig. S4. Exponential fit to the adaptation to standard and deviant tone does not alone explain SSA maturation. (**A, B**) Exponential fits (see STAR methods) of the normalized average firing rate for each standard (A) and deviant tone (B) across sessions for the different ages and areas. Color code as in Fig. 1. (**C**) Average coefficient a values of the fits to the standard (upper panel)

or deviant (lower panel) responses across ages and areas. ***, $p<0.001$; n.s., $p>0.05$. Ordinary One-way ANOVA with multiple comparisons. (**D**) Average tau value of the fits to the standard (upper panel) or deviant (lower panel) responses across ages and areas. ***, $p<0.001$; n.s., $p>0.05$. Ordinary One-way ANOVA with multiple comparisons The violin plots represent the median in the bigger dashed line and the 25th and 75th percentiles in the smaller dashed lines. (**E**) Average CSI for ICC (left), MGV (middle) and A1 (right), where the first repetitions of each sequences (out of 15 repetitions in total, corresponding to 65 tones or to the first 22.7s of each session) have been omitted. ICC: P20, 5 mice, 72 units; P30, 5 mice, 44 units; P40, 5 mice, 106 units; P50, 6 mice, 83 units; f=0.31, df=304. MGV: P20, 5 mice, 140 units; P30, 6 mice, 90 units; P40, 5 mice, 93 units; P50, 5 mice, 42 units; f=12.58, df=364. A1: P20, 7 mice, 97 units; P30, 6 mice, 186 units; P40, 5 mice, 154 units; P50, 7 mice, 182 units; f=25.07, df=618. One-way ANOVA with multiple comparisons. n.s., $p\geq0.05$; ***, $p<0.001$. Ordinary One-way ANOVA with multiple comparisons. In the boxplots, lines represent median, 25th and 75th percentiles, + represents mean, whiskers represent 10th and 90th percentiles, and points below or above the whiskers are drawn as individual points.

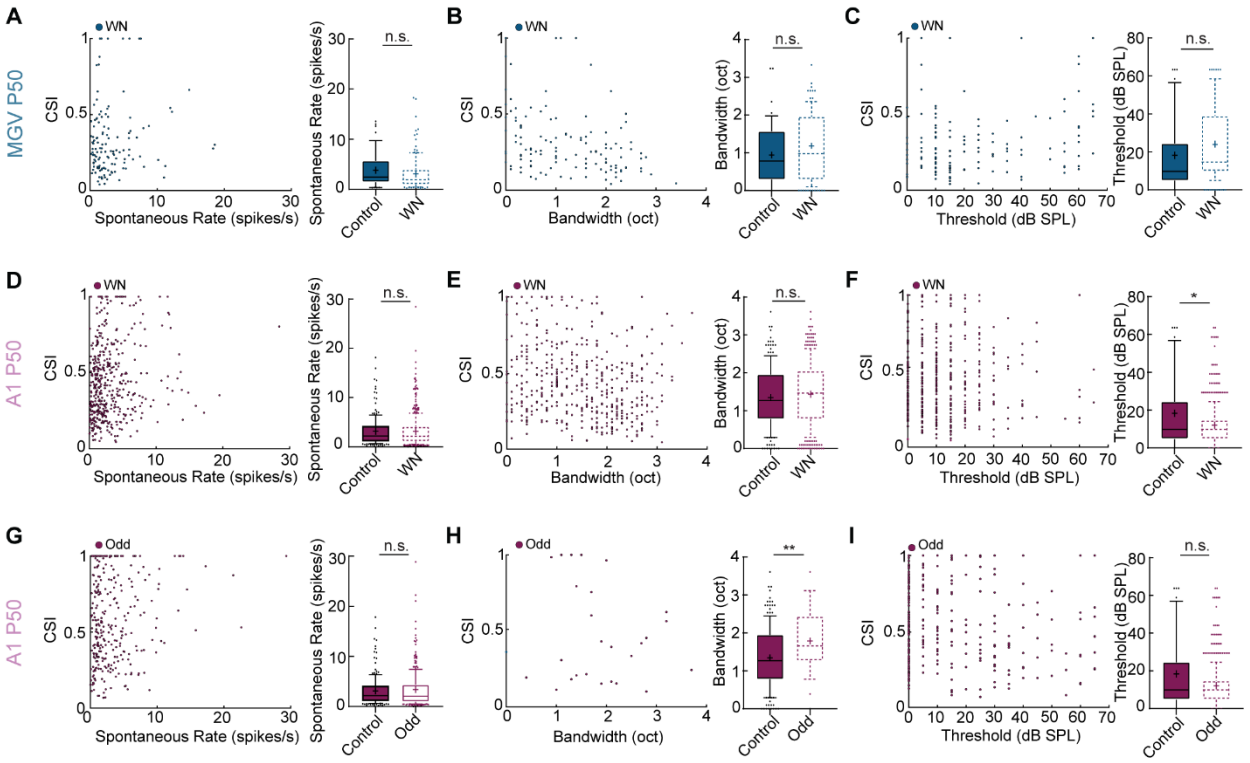

Fig. S5. A1 experience-dependent changes do not correlate with spontaneous rate, response bandwidth, or threshold. (**A**) Left: Scatter plot of CSI vs. spontaneous rate for WN-exposed MGV P50 mice. Right: Comparison of spontaneous rate in control vs. WN-exposed mice. n.s., p≥0.05. (**B**) Left: Scatter plot of CSI vs. bandwidth for WN-exposed MGV P50 mice. Right: Comparison of bandwidth in control vs. WN-exposed mice. n.s., p≥0.05. (**C**) Left: Scatter plot CSI vs. threshold for WN-exposed MGV P50 mice. Right: Comparison threshold control vs. WN-exposed mice. n.s., p≥0.05. (**D**) Same as (A) for WN-exposed A1 P50 mice. n.s., p≥0.05. (**E**) Same as (B) for WN-exposed A1 P50 mice. n.s., p≥0.05. (**F**) Same as (C) for WN-exposed A1 P50 mice. p=0.035. (**G**) Same as (A) for WN-exposed A1 P50 mice. n.s., p≥0.05. (**H**) Same as (B) for Odd-exposed A1 P50 mice. p=0.009. (**I**) Same as (C) for WN-exposed A1 P50 mice. Unpaired student t-test. Data represent mean ± SEM**.** In the boxplots, lines represent median, 25th and 75th percentiles, + represents mean, whiskers represent 10th and 90th percentiles, and points below or above the whiskers are drawn as individual points. See also Table S1.

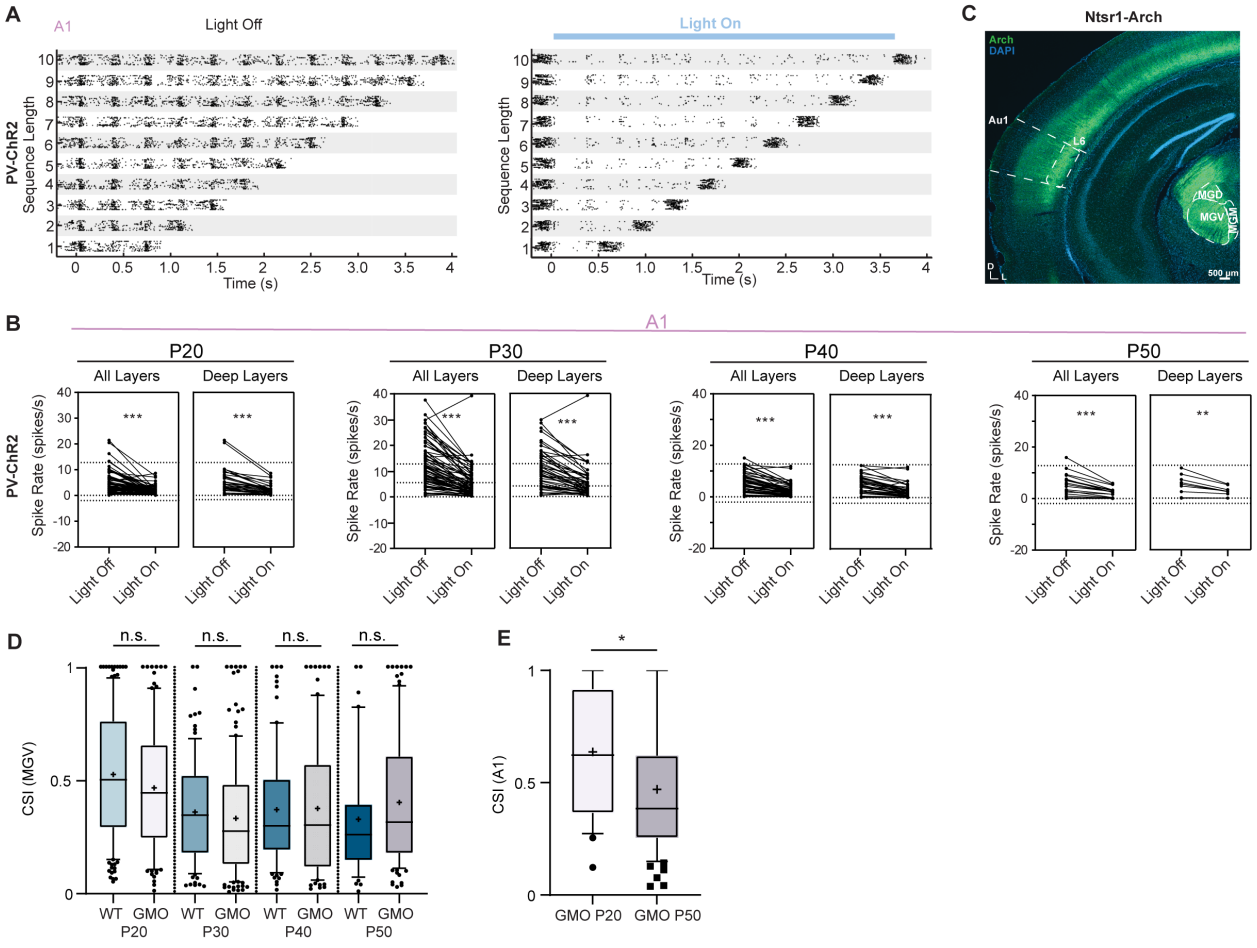

Fig. S6. A1 silencing strongly decreases CSI in MGV across adolescence. (**A**) Representative Raster plot of an A1 PV$^-$- cell's response to the 10 oddball sequences without the light (left) and with the light on (right, the timeline for the light on applies for the top sequence). (**B**) Average spike rates of A1 neurons without the light (light off) and with the light on across age for neurons situated in all layers (P20, 74 cells; P30, 70 cells; P40, 62 cells; P50, 18 cells) or in deep layers only (P20, 33 cells; P30, 45 cells; P40, 40 cells; P50, 9 cells). ***, p<0.0001; **, p=0.005, paired-student t-test. (**C**) Representative left hemisphere coronal slice of P40 mouse (bregma -2.92 mm). A1 and MGV highlighted (dashed white lines). Arch expression in A1 L6 projections to MGB confirmed using antibody against GFP (green). Cell nuclei stained with DAPI (blue). 10x magnification. 500 µm scale. MGD, dorsal MGB; MGM, medial MGB. Au1, primary auditory cortex. Layer 6, L6. (**D**) CSI values in the MGB for WT and PV-ChR2 mouse lines at all ages (WT, n as in Fig. 1I; genetically modified organism (GMO) n=101 (P20), 142 (P30), 80 (P40), 105(P50)). n.s., p=0.104 (P20), 0.383 (P30), 0.897 (P40), 0.144 (P50), unpaired student t-test. (**E**) CSI values in A1 for PV-ChR2 mice at P20 (n= 25) and P50 (n=68), *, p=0.014, unpaired student t-test.

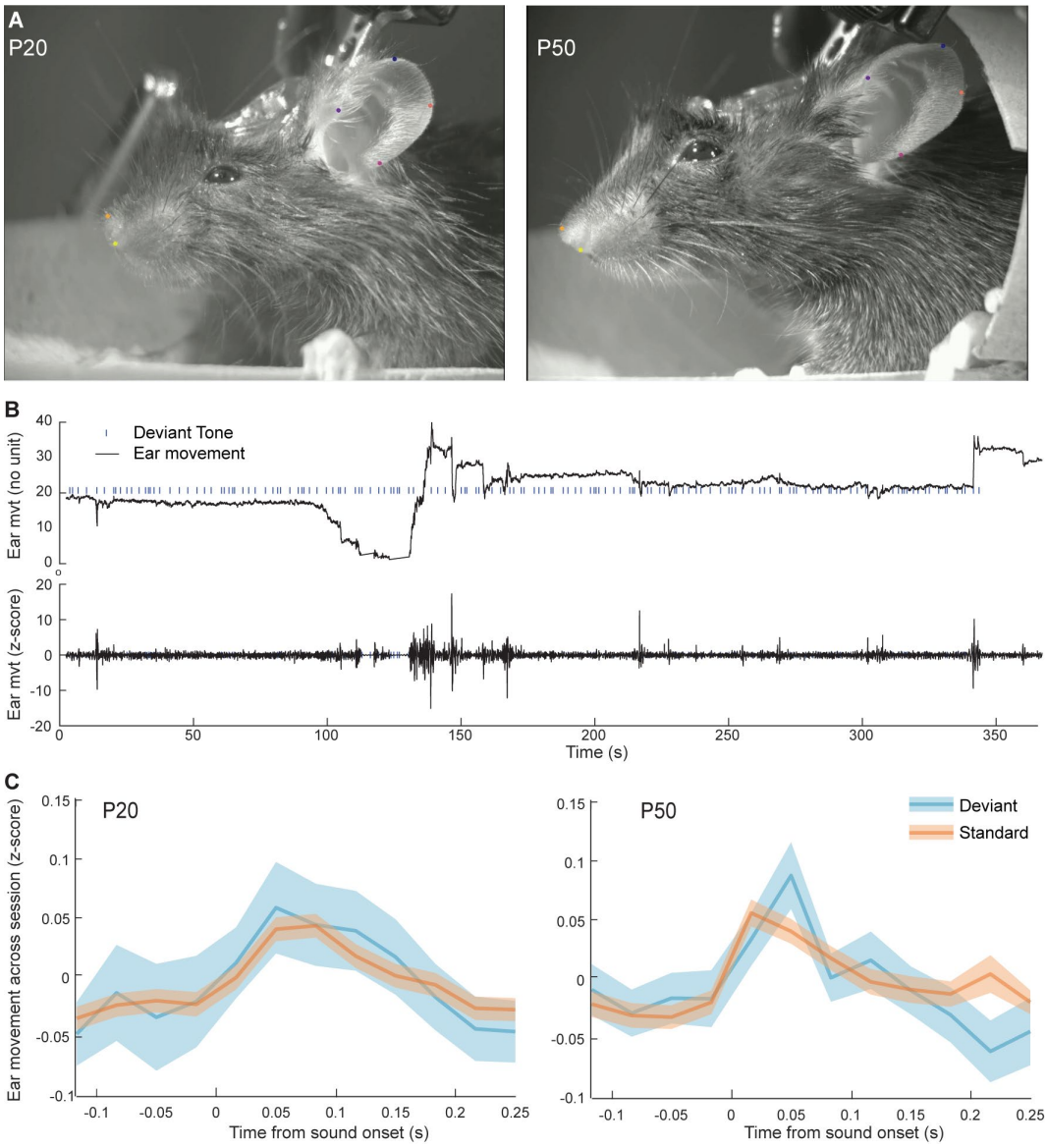

Fig. S7. Tracking the movement of the ear in response to sound stimuli. (A) Example frames from videos taken in a P20 (left) and a P50 (right) mouse, with dots used to track body movements. (**B**) Example trace obtained with deep lab cut referring to the movement in the y direction of the point at the top of the ear in (A) across a recording session. The blue lines indicate the time of the deviant tone presentations (upper trace). High-pass filtered and z-score equivalent of the upper trace (lower trace). (**C**) z-scored ear-movement aligned to the onset of standard (orange) or deviant (blue) tones, averaged across 5 animals and 2 sessions in each, for P20 (left) and P50 (right mice). The statistical comparison of pre- and post-stimulus indicates significant differences (P20 standard tone: $p<0.0001$, P20 deviant tone, $p<0.0001$; P50 standard tone: $p<0.0001$, P50 deviant tone, $p<0.0001$, Wilcoxon signed-rank test), but the comparison of deviant versus standard indicates no significant difference (P20, $p=0.1925$; P50, $p=0.3533$, Wilcoxon rank sum test). The pre-stimulus window is from -100 ms to 0 ms, and the post-stimulus window from 0 to 100 ms after tone onset.

Figure panel	Conditions		Correlation		
			r	R squared	p
Fig. 3B	ICC	P20	-0.0952	0.0091	0.4296
		P30	0.6240	0.3900	0.0001
		P40	0.1220	0.0149	0.2132
		P50	0.1960	0.0384	0.0775
	MGV	P20	-0.2720	0.0738	0.0012
		P30	-0.0660	0.0044	0.5250
		P40	0.0273	0.0007	0.8021
		P50	-0.0308	0.0009	0.8448
	A1	P20	-0.1150	0.0133	0.2641
		P30	-0.0992	0.0098	0.1817
		P40	0.0001	0.0000	0.9985
		P50	0.0499	0.0025	0.5025
Fig. 3D	ICC	P20	-0.0407	0.0017	0.7358
		P30	-0.1700	0.0289	0.2700
		P40	0.0250	0.0006	0.7993
		P50	0.0475	0.0023	0.6718
	MGV	P20	-0.0140	0.0002	0.8705
		P30	-0.1070	0.0114	0.3039
		P40	-0.1500	0.0224	0.1662
		P50	0.0837	0.0070	0.5935
	A1	P20	0.0510	0.0026	0.6160
		P30	-0.2380	0.0566	0.0013
		P40	-0.0287	0.0000	0.7265
		P50	-0.2180	0.0005	0.7726
Fig. 3F	ICC	P20	0.1010	0.0102	0.4009
		P30	-0.3280	0.1070	0.0299
		P40	-0.0691	0.0048	0.4815
		P50	-0.3150	0.0990	0.0040
	MGV	P20	-0.0600	0.0036	0.4816
		P30	0.0982	0.0096	0.3439
		P40	-0.0873	0.0076	0.4213
		P50	-0.0471	0.0022	0.7641
	A1	P20	0.1440	0.0208	0.1612
		P30	0.0027	0.0007	0.9797
		P40	0.1680	0.0281	0.0376
		P50	-0.1620	0.0263	0.0282
Fig. S5A	MGV	WN	0.1110	0.0123	0.2064
S5B			-0.3730	0.1390	0.0001
S5C			0.2430	0.0589	0.0051
Fig. S5D	A1	WN	0.1470	0.0216	0.0018
S5E			-0.210	0.0439	0.0001
S5F			-0.0284	0.0008	0.5490
Fig. S5G	A1	Odd	0.1250	0.0155	0.0294
S5H			-0.1320	0.0173	0.5130
S5I			-0.2170	0.0472	0.0001

Table S1. Statistical tests. The Pearson coefficient (r) and p-value (p; two-tailed) represent a negative ($r<0$, $p<0.05$), positive ($r>0$, $p<0.05$), or no correlation between CSI and the functional properties of the auditory neurons. Top to bottom: Control groups spontaneous activity (Fig. 3B), bandwidth at 60 dB SPL (Fig. 3D) and threshold (Fig. 3F); Exposed groups spontaneous activity (Fig. S5A, D and G), bandwidth (Fig. S5B, E and H) and threshold (Fig. S5C, F and I).